

A Comparative Study on Dry Sliding Wear Characteristics of Al₂O₃ and Bone Powder Filled Hybrid Composites

Sudeep Deshpande^{1*}, T. Rangaswamy²

¹Department of Mechanical Engineering, SKSVMACET, Laxmeshwar, India

²Department of Mechanical Engineering, G. E. C., Hassan, India

Email: ^{*}sudeepmech@yahoo.com

Received 16 February 2016; accepted 27 March 2016; published 30 March 2016

Copyright © 2016 by authors and Scientific Research Publishing Inc.

This work is licensed under the Creative Commons Attribution International License (CC BY).

<http://creativecommons.org/licenses/by/4.0/>



Open Access

Abstract

The aim of the research was to develop E-glass/jute fiber reinforced epoxy composites with an addition of Al₂O₃ and bone powder by using hand layup technique and to compare tribological properties of these composites under similar test conditions. The wear experiments were designed according to Taguchi's (L₂₇) orthogonal array with three control variables such as sliding velocity, filler content and normal load. The results indicated that the normal load for Al₂O₃ and filler content for bone powder emerged as the significant factors affecting specific wear rate of hybrid composites. An addition of 10 wt% of bone powder or Al₂O₃ into E-glass/jute fiber reinforced epoxy composites increased the wear resistance considerably, and natural waste bone powder can be used instead of ceramic filler Al₂O₃ in hybrid composites. After the analysis of control factors, an optimal factor setting has been suggested for specific wear rate and coefficient of friction. Further, the scanning electron microscopy (SEM) images for worn surfaces of hybrid composites were studied. Finally, a confirmation test was carried out to validate the results.

Keywords

Al₂O₃, Bone Powder, Wear Test, Taguchi Analysis, SEM

1. Introduction

Composite materials can be described as engineering or naturally occurring materials made from two or more constituent materials with essentially different physical or chemical properties which remain separate and dis-

*Corresponding author.

tinct at the macroscopic or microscopic scale within the finished structure [1]. As polymers can be filled with organic fillers and inorganic fillers, inorganic-filled composites have become attractive in polymer field due to its various advantages such as easiness in processing, cost effectiveness and excellent performance over the metals. Polymer composites have a special property of self lubrication and this made the composites suitable in tribological applications such as cams, seals, brakes, bearings etc. [2].

Many researchers showed interest in developing the new natural fiber composites because of their low cost, combustibility, lightweight, low density, high specific strength, renewability, non-abrasivity, non-toxicity and biodegradability [3]-[5]. Natural fibers are renewable and biodegradable materials and are largely available in worldwide nature [6]-[8]. Pine, apple leaf, oil palm fiber, hemp, sisal, jute, kapok, rice husk, bamboo and wood are the fibers most commonly used as reinforcing natural fibers in polymer matrix [9]-[11]. Nowadays, in the field of composites, waste material is used as a filler like eggshell, uncarbonized bone and carbonized bone powder. Eggshell contains about 95% calcium carbonate in the form of calcite and 5% organic materials such as type X collagen, sulfated polysaccharides and other proteins [12]. Filler materials are used to reduce the material costs, to improve mechanical properties to some extent and in some cases to improve process ability. It also increases properties like abrasion resistance, hardness and reduce shrinkage. Properties of composites are strongly dependent on the properties of their constituent materials, their distribution and the interaction among them. The geometry of the reinforcement (shape, size and size distribution) influences the properties of the composite to a great extent. Natural fibers and glass fibers, reinforced thermoplastic composite, have successfully proven their high qualities in various fields of technical application. Natural fibers used as replacements for aramid and glass fibers due to their low density, good thermal insulation and mechanical properties, reduced tool wear, unlimited availability, low price, and problem free disposal. In view of the above, an attempt was made to study the effect of Al_2O_3 and bone powders as a filler material in E-glass/jute epoxy composite. The wear characteristics of these hybrid composites were investigated and analyzed.

2. Experimental Details

2.1. Materials

In this work, 7-mil E-glass fibers, woven jute fibers, epoxy L-12 (3202) and K-6 hardener were used for fabricating the composite materials [13] [14]. Aluminium oxide particles size was 70 - 230 mesh and uniformly distributed throughout the matrix. The average density of aluminium oxide was 3.89 g/cc. Goat bones were washed and cleaned. Goat bone powder was used as filler material since eggshell and bone belong to the same calcium group [12]. Thin top surface layer of the bone was removed by using grinding machine and powder was prepared. An approximate density value of bone powder was 1.95 g/cc.

2.2. Fabrication and Specimen Preparation of Hybrid Composites

The hybrid fiber reinforced epoxy composites were prepared by keeping constant 40 wt% of E-glass fiber and 10 wt% of jute fiber. The composites filled with varying concentrations (0 wt%, 10 wt% and 15 wt%) of Al_2O_3 and bone powder were fabricated by using hand layup technique [15]. Jute plies were placed in between E-glass plies and also E-glass plies were placed at extreme ends of the composites. The epoxy, hardener and fillers were mixed in a basin and the mixture was subsequently stirred constantly till the filler was uniformly distributed throughout the mixture [16]. The plies was placed one above the other and the epoxy mixture was brushed uniformly over the woven E-glass and the woven jute plies. Care was taken that the plies were properly coated with epoxy mixture. Entrapped air was removed manually with squeezers or rollers to complete the composite structure. The composites were put under load for about 24 hours for proper curing at room temperature. The fabricated hybrid composites were taken out from the mould and then specimens were prepared according to ASTM G99 standards. The composites were cut by using Zigzag board cutter machine. Three identical test specimens were prepared for each test.

2.3. Density Test

The theoretical density (ρ_t) of hybrid composite material in terms of weight fractions of different constituents can be obtained from the following Equation (1) [17].

$$\rho_t = \frac{1}{\left(\frac{W_g}{\rho_g}\right) + \left(\frac{W_j}{\rho_j}\right) + \left(\frac{W_m}{\rho_m}\right) + \left(\frac{W_f}{\rho_f}\right)} \quad (1)$$

where, W and ρ represent the weight fraction and density respectively. The suffixes g, j, m and f stand for the E-glass fiber, jute fiber, matrix (epoxy) and filler respectively.

The actual density (ρ_e) of the composites can be determined experimentally by simple water immersion technique. The volume fraction of voids (V_v) in the composites was calculated using the following Equation (2) [17].

$$V_v = \frac{(\rho_t - \rho_e)}{\rho_t} \quad (2)$$

2.4. Brinell Hardness Test

Brinell hardness test was conducted on the specimen using a standard Brinell hardness tester [18]. A load of 2500 N was applied on the specimen for 30 sec using 5 mm diameter hard metal ball indenter and the indentation diameter was measured using a microscope. The hardness was measured at three different locations of the specimen and the average value was calculated as shown in Table 2 [19].

2.5. Dry Sliding Wear Test Apparatus

DUCOM pin on disc test apparatus was used to investigate the dry sliding wear characteristics of hybrid composites. The disc made of hardened EN-31 hardened ground steel to 62 HRC, surface roughness 1.6 μm Ra, 120 mm track diameter and 8 mm thick. Specimen with size of 10 mm \times 10 mm \times 30 mm was subjected vertically to the counter face where the contact area was constant. Wear test was carried out for constant sliding distance of 2000 m, sliding velocities of 1.4 m/sec, 2 m/sec and 2.6 m/sec against the normal loads of 20 N, 40 N, and 60 N and wear rate data reported was the average of two runs. Care was to see that the specimen was continuously cleaned with woolen cloth to avoid the entrapment of wear debris and to achieve uniform experimental procedure. After each test the disc was cleaned using acetone solution. The initial weight before run and final weight after run was measured using a precision electronic balance with an accuracy of ± 0.01 mg.

The specific wear rate (mm^3/Nm) was then expressed on volume loss basis as shown below Equation (3) [20].

$$K_s = \frac{\Delta m}{\rho t v F} \quad (3)$$

where, K_s = Specific wear rate (mm^3/Nm); Δm = Mass loss (gms); ρ = Density of specimen (g/cc); t = Test duration (sec); v = sliding velocity (m/s); F = Applied load (N).

2.6. Taguchi Experimental Design

Taguchi technique was used for analyzing the influence of control factors on performance output [21] [22]. The most important stage in the design of experiment lies in the selection of control factors. In the present work, the impact of three parameters such as sliding velocity, normal load and filler content were studied using L_{27} (3^{13}) Taguchi orthogonal design [23]. The experimental results were transformed into a signal-to-noise (S/N) ratio. The S/N ratio for minimum wear rate coming under “smaller is better” characteristic, and it was calculated as logarithmic transformation of the loss function as shown below Equation (4) [1].

$$\frac{S}{N} = -10 \log \left[\frac{1}{n} (y_1^2 + y_2^2 + \dots + y_n^2) \right] \quad (4)$$

where n indicates the repeated number of trial conditions; y_1, y_2, \dots, y_n indicates the response of the dry sliding wear characteristics respectively. For “Lower is better” (LB) characteristic of the above S/N ratio transformation, it was suitable for minimizations of coefficient of friction and specific wear rate. The standard linear graph was used to assign the factors and interactions to various columns of the orthogonal array.

The plan of the experiments: The experiments were conducted as per the standard orthogonal array L_{27} (3^{13}). The selection of the orthogonal array was based on the condition that the degree of freedom for the orthogonal

array should be greater than or equal to the sum of those wear parameters.

In the present investigation L_{27} Taguchi orthogonal array was chosen and this has 27 rows and 13 columns. The wear parameters chosen were: 1) sliding velocity; 2) normal load and 3) filler content, and their levels are indicated in **Table 1**. The experiments consisted of 27 tests (each row in the L_{27} orthogonal array) and were assigned with parameters. The first column in the table was assigned to sliding velocity (S); the second column was assigned to normal load (L); the fifth column was assigned to filler content (FC) and the remaining columns were assigned to their interactions. The dry sliding wear tests result were subjected to the analysis of variance.

3. Results and Discussion

3.1. Density

In the present research work, the theoretical and experimental densities of hybrid composites along with the corresponding volume fraction of voids are presented in **Table 2**. It was found that the composite density values calculated theoretically from weight fractions were not equal to the experimentally measured values. It was evident from **Table 2** that the density values for hybrid composites increase with the addition of filler content. It was further observed that with the incorporation of fillers, the void fractions in these composites also increase. As similar observation has been reported earlier for hybrid composite filled with different filler content [24].

3.2. Wear Behavior of Bone Powder Filled Hybrid Composites

The experimental data for specific wear rate and coefficient of friction of bone powder filled hybrid composites reported in **Table 3**. The overall mean for the S/N ratio of the specific wear rate and the coefficient of friction were found to be 91.995 db and 7.105 db respectively.

3.2.1. ANOVA and Effects of Factors on Specific Wear Rate

It was observed that the filler content (C) factor ($P = 44.25\%$), normal load (B) factor ($P = 16.67\%$) and the interaction between sliding velocity \times filler content ($P = 10.51\%$) have great influence on the specific wear rate and hence these were physically and statistically highly significant from the ANOVA **Table 4**. However interaction (A \times B) between sliding velocity \times normal load ($P = 9.09\%$), interaction between normal load \times filler content ($P = 7.57\%$) and sliding velocity (A) factor ($P = 1.10\%$) have lesser effect on specific wear rate as error value ($P = 10.87$) was higher side hence less significant. From the analysis of ANOVA and response **Table 5** of

Table 1. Levels of variables used in the experiments.

Control factor	Symbols	Level			Units
		I	II	III	
Sliding Velocity	A	1.4	2	2.6	m/s
Normal Load	B	20	40	60	N
Filler Content	C	0	10	15	%

Table 2. Theoretical and experimental densities of hybrid composites.

Hybrid Composites	Theoretical Density in gm/cc	Experimental Density in gm/cc	Volume Fraction of voids in %	Brinell Hardness Number (BHN) [18] [19]
GJE	1.6183	1.5621	3.47	55.25
GJEA1	1.7684	1.6816	4.90	34.85
GJEA2	1.8573	1.7584	5.33	68.39
GJEB1	1.6919	1.6255	3.92	30
GJEB2	1.7312	1.6120	6.88	57.1

G: E-glass fibers; J: Jute fibers; A: Al_2O_3 ; B: Bone Powder; 1: 10 wt%; 2: 15 wt%.

Table 3. Experimental design using L₂₇ array for Al₂O₃ and bone powder filled hybrid composites.

S. No	Sliding Velocity (S) in m/s	Normal Load (L) in N	Filler Content (FC) in %	Specific Wear Rate (W) in mm ³ /Nm	S/N Ratio (db)	Coefficient of Friction (μ)	S/N Ratio (db)
1	1.4	20	GJE	8.01E-05	81.93	0.396	8.046
2			GJEB1	1.58E-05	96.05	0.593	4.539
3			GJEA1	5.06E-05	85.917	0.274	11.2450
4		GJEB2	1.58E-05	96.02	0.195	14.199	
5		GJEA2	0.0001081	79.323	0.441	7.1112	
6		GJE	7.20E-05	82.85	0.427	7.391	
7		GJEB1	7.88E-06	102.07	0.528	5.547	
8		GJEA1	7.60E-05	82.384	0.384	8.3134	
9		GJEB2	5.53E-05	85.14	0.37	8.636	
10	2	40	GJEA2	2.70E-05	91.373	0.444	7.0523
11			GJE	4.27E-05	87.39	0.48	6.375
12			GJEB1	1.58E-05	96.05	0.636	3.931
13		GJEA1	1.13E-05	98.938	0.432	7.2903	
14		GJEB2	2.11E-05	93.52	0.414	7.660	
15		GJEA2	3.60E-05	88.874	0.421	7.5144	
16		GJE	7.99E-05	81.95	0.369	8.659	
17		GJEB1	1.57E-05	96.07	0.612	4.265	
18		GJEA1	5.05E-05	85.931	0.304	10.3425	
19	2.6	20	GJEB2	6.31E-05	84.00	0.507	5.900
20			GJEA2	7.19E-05	82.868	0.629	4.0270
21			GJE	3.99E-05	87.97	0.452	6.897
22		GJEB1	1.57E-05	96.07	0.675	3.414	
23		GJEA1	8.42E-06	101.494	0.314	10.0614	
24		GJEB2	1.58E-05	96.04	0.398	8.002	
25		GJEA2	4.49E-05	86.950	0.385	8.2908	
26		GJE	3.73E-05	88.57	0.293	10.663	
27		GJEB1	1.05E-05	99.60	0.467	6.614	
28	20	60	GJEA1	1.12E-05	98.995	0.348	9.1684
29			GJEB2	1.58E-05	96.04	0.352	9.069
30			GJEA2	4.19E-05	87.549	0.573	4.8369
31	2.6	20	GJE	6.41E-05	83.86	0.366	8.730
32			GJEB1	4.73E-05	86.50	0.689	3.236
33			GJEA1	1.69E-05	95.442	0.225	12.9563
34	2.6	20	GJEB2	3.17E-05	89.99	0.37	8.636
35			GJEA2	5.41E-05	85.335	0.6	4.4370

Continued

22		GJE	4.81E-05	86.36	0.437	7.190
23		GJEB1	7.89E-06	102.06	0.617	4.194
	40	GJEA1	2.54E-05	91.920	0.383	8.3360
24		GJEB2	7.91E-06	102.03	0.339	9.396
	2.6	GJEA2	2.71E-05	91.356	0.526	5.5803
25		GJE	2.67E-05	91.46	0.479	6.393
26		GJEB1	3.68E-05	88.68	0.637	3.917
	60	GJEA1	1.69E-05	95.442	0.332	9.5772
27		GJEB2	5.28E-06	105.55	0.304	10.343
		GJEA2	1.80E-05	94.878	0.448	6.9744

Table 4. ANOVA table for specific wear rate of bone powder filled hybrid composites.

Source	DF	Seq SS	Adj SS	Adj MS	Test F	P (%)
A	2	1.50	1.498	0.75	0.38	1.05
B	2	23.89	23.89	11.95	6.13	16.67
C	2	63.41	63.41	31.71	16.26	44.25
A * B	4	13.02	13.02	3.26	1.67	9.09
A * C	4	15.06	15.06	3.77	1.93	10.51
B * C	4	10.84	10.84	2.71	1.39	7.57
Residual Error	8	15.57	15.57	1.95		10.87
Total	26	143.29				100.00

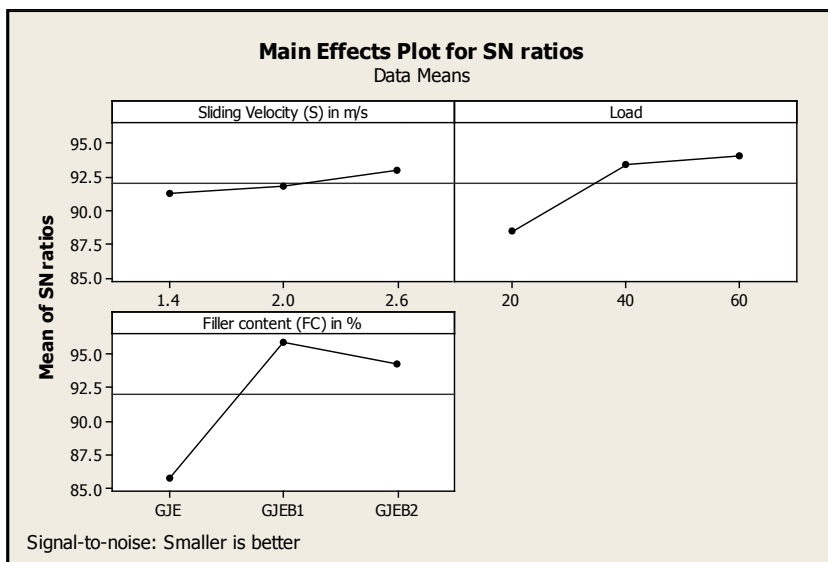
DF—degree of freedom; Seq SS—sequential sum of squares; Adj SS—extra sum of squares; Seq MS—sequential mean squares; F—F-test and P—percent contribution.

Table 5. Response table for specific wear rate of bone powder filled hybrid composites.

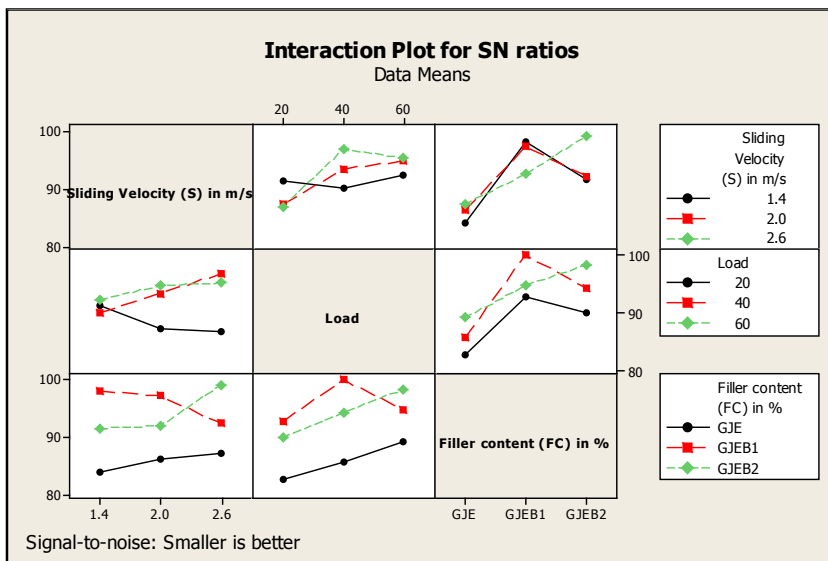
Level	Control Factors		
	A	B	C
1	91.23	88.49	85.82
2	91.81	93.4	95.91
3	92.95	94.1	94.26
Delta	1.72	5.61	10.09
Rank	3	2	1

the S/N ratio for specific wear rate as shown in Figure 1(a), it was observed that the filler content has major impact on specific wear rate followed by normal load and sliding velocity.

The influence of each control factor (sliding velocity, normal load and filler content) on the specific wear rate was analyzed with a main effect plot as shown in Figure 1(a) and an interaction plot as shown in Figure 2(b). From the analysis of ANOVA and response Table 5 of the S/N ratio for specific wear rate, it was observed that the control factor filler content (C) has major impact on the specific wear rate followed by the normal load (B) and sliding velocity (A). It means that for bone powder filled hybrid composites with the increase of the filler



(a)



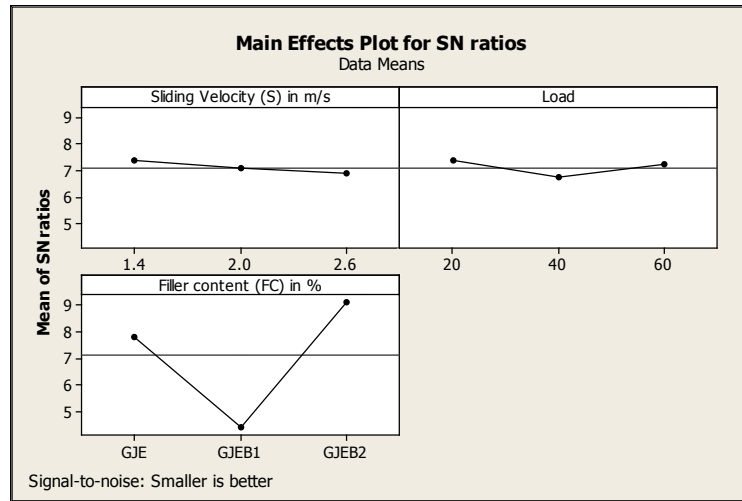
(b)

Figure 1. Effect of (a) control factors; (b) Interaction of factors on specific wear rate of bone powder filled hybrid composites.

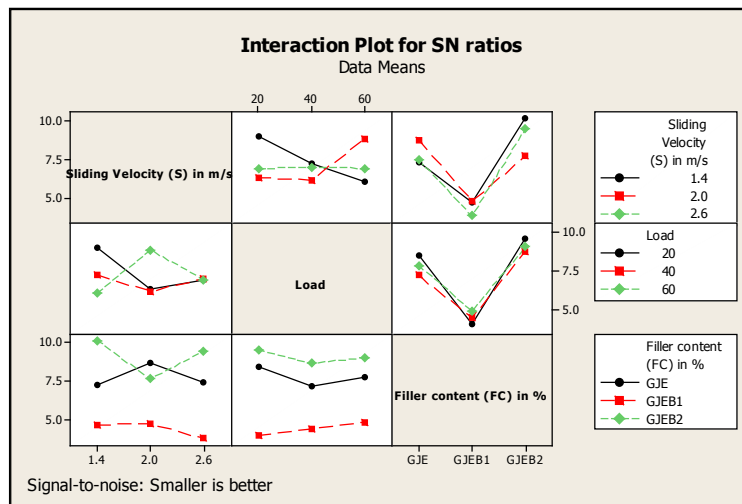
content, sliding velocity and normal load the specific wear rate decreases i.e., good wear resistance. It was also observed that the filler content plays adverse effect, when the filler content was increased from 0 wt% to 10 wt% the specific wear rate was decreased due to good bonding strength between the fibers, filler and matrix. When the filler content was increased from 10 wt% to 15 wt% specific wear rate was increased due to presence of voids, weak bonding strength between fiber and matrix. The experimental results show that further increase in filler content increases specific wear rate [12]. Analysis of these results leads to the conclusion that optimal values of the parameters for minimizing the wear rate when the sliding velocity and normal load were at level 3 and the filler content was at level 2.

3.2.2. ANOVA and Effects of Factors on Coefficient of Friction

ANOVA **Table 6** for the coefficient of friction that the filler content factor ($P = 69.33\%$), interaction between sliding velocity \times normal load ($P = 12.62\%$) and the interactions between sliding velocity \times filler content ($P =$



(a)



(b)

Figure 2. Effect of (a) control factors; (b) Interaction on COF of bone powder filled hybrid composites.

Table 6. ANOVA table for COF of bone powder filled hybrid composites.

Source	DF	Seq SS	Adj SS	Adj MS	Test F	P (%)
A	2	0.00900	0.00900	0.00450	1.52718	2.07
B	2	0.00022	0.00022	0.00011	0.03733	0.05
C	2	0.30110	0.30110	0.15055	51.09278	69.33
A * B	4	0.05480	0.05480	0.01370	4.64943	12.62
A * C	4	0.02850	0.02850	0.00713	2.41804	6.56
B * C	4	0.01711	0.01711	0.00428	1.45167	3.94
Residual Error	8	0.02357	0.02357	0.00295		5.43
Total	26	0.43430				100.00

DF—degree of freedom; Seq SS—sequential sum of squares; Adj SS—extra sum of squares; Seq MS—sequential mean squares; F—F-test and P—percent contribution.

6.56%) have significant influence on the coefficient of friction. However interaction of normal load x filler content ($P = 3.94\%$), sliding velocity ($P = 2.07\%$) and normal load factor ($P = 0.05\%$) do not have a significant effect (both physically and statistical) on coefficient of friction as their values are quite smaller than error ($P = 5.43\%$). So they were neglected. From the analysis of ANOVA and response **Table 7** of the S/N ratio of coefficient of friction, it was observed that the control parameter filler content (C) has a major impact on coefficient of friction followed by normal load and sliding velocity.

The influence of each control factor on the coefficient of friction was analyzed with a main effect plot as shown in **Figure 2(a)** and an interaction plot as shown in **Figure 2(b)**. From the analysis of ANOVA and response **Table 7** of the S/N ratio for coefficient of friction, it was observed that the control factor filler content (C) has major impact on the coefficient of friction. It means that for bone powder filled hybrid composites, with the increases of the filler content from 0 wt% to 10 wt%, coefficient of friction increases and from 10 wt% to 15 wt% coefficient of friction decreases. The same trend was observed for normal load. Analysis of these results leads to the conclusion that optimal values of the parameters for minimizing the coefficient of friction when the sliding velocity and normal load were at level 1 and the filler content was at level 3.

3.2.3. Surface Morphology of Bone Powder Filled Hybrid Composites

When compared with sliding velocity and normal load the effect of filler content on specific wear rate was more as seen from the main effect plot as shown in **Figure 1(a)**. For analysis, varying concentration of filler content composite samples were selected and at 20N normal load condition. The micrograph in **Figure 3(a)** unfilled hybrid composite show the wedge formation, fiber exposure and plastic deformation of matrix which results maximum wear. The SEM image as shown in **Figure 3(b)** 10 wt% of bone powder filled hybrid composite illustrate only a few fibers exposure when compared with **Figure 3(a)** and less deformation of the matrix which indicates less wear. **Figure 3(c)** 15 wt% of bone powder filled hybrid composite show more plastic deformation of the matrix which slightly increases the wear rate when compared with **Figure 3(b)**.

Similarly, coefficient of friction was affected by filler content as seen from the main effect plot **Figure 2(a)**. So SEM images were selected for varying concentration of filler content of hybrid composites. The worn surface of **Figure 3(d)** unfilled hybrid composite and **Figure 3(f)** 15 wt% of bone powder filled hybrid composite show the wear track, minor crack and only few fibers exposed from the matrix which has less coefficient of friction. The SEM image for **Figure 3(e)** 10 wt% of bone powder filled hybrid composite sample show the wear track on the surface, breakage of fibers and more number of fibers exposed which increased the coefficient of friction due to the rubbing action of the fibers with the disc surface.

3.3. Wear Behavior of Aluminium Oxide (Al_2O_3) Filled Hybrid Composites

The experimental data for specific wear rate and coefficient of friction of aluminium oxide (Al_2O_3) filled hybrid composite reported in **Table 3**. The overall mean for the S/N ratio of the specific wear rate and the coefficient of friction were found to be 88.789 db and 7.905 db respectively.

3.3.1. ANOVA and Effects of Factors on Specific Wear Rate

It was observed that from the ANOVA **Table 8** the normal load (B) factor ($P = 37.64\%$) and filler content (C) factor ($P = 17.63\%$) have great influence on the specific wear rate and hence these were physically and statisti-

Table 7. Response table for COF of bone powder filled hybrid composites.

Level	Control Factors		
	A	B	C
1	7.369	7.357	7.816
2	7.054	6.741	4.406
3	6.893	7.218	9.093
Delta	0.477	0.616	4.687
Rank	3	2	1

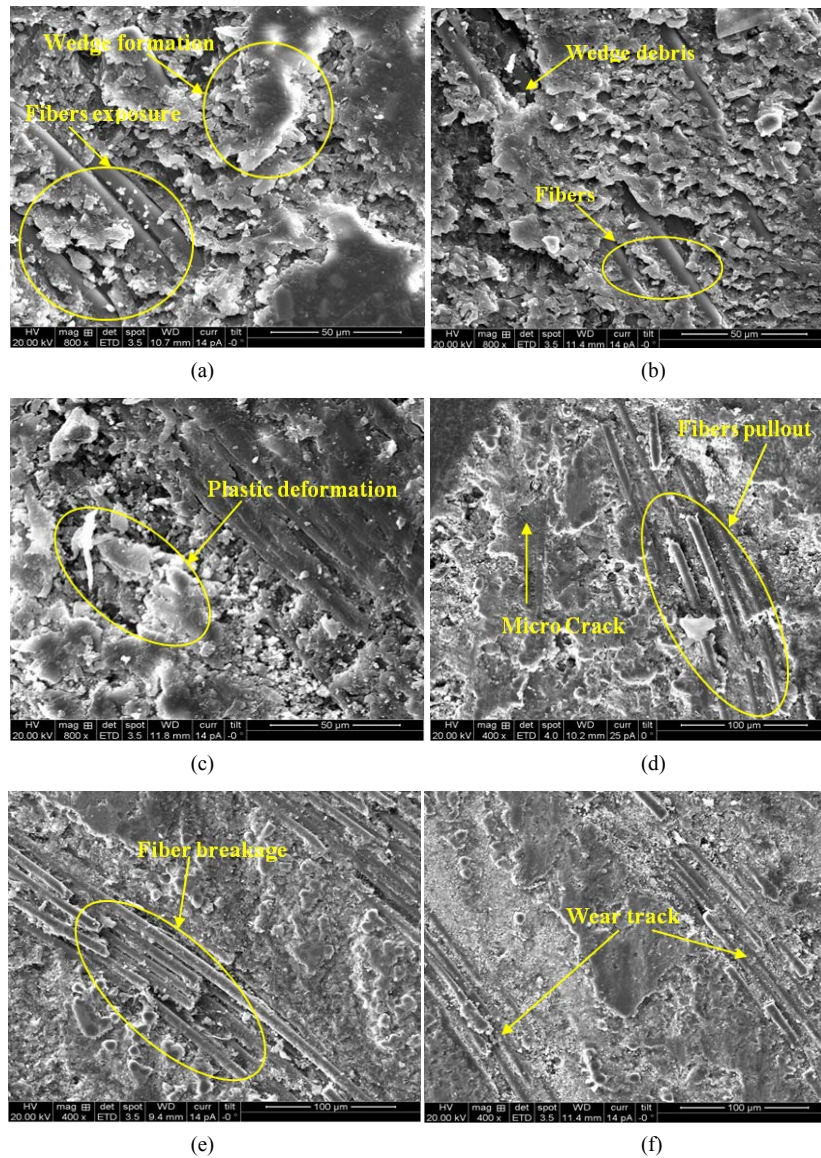


Figure 3. SEM images of composites for bone powder filled hybrid composites.

Table 8. ANOVA table for specific wear rate of Al_2O_3 filled hybrid composites.

Source	DF	Seq SS	Adj SS	Adj MS	Test F	P (%)
A	2	23.85	23.85	11.925	3.9883	14.19
B	2	63.25	63.25	31.625	10.5769	37.64
C	2	29.62	29.62	14.810	4.9532	17.63
A*B	4	10.06	10.06	2.515	0.8411	5.99
A*C	4	3.55	3.55	0.888	0.2968	2.11
B*C	4	13.75	13.75	3.438	1.1497	8.18
Residual Error	8	23.94	23.94	2.993		14.25
Total	26	168.02				100.00

DF—degree of freedom; Seq SS—sequential sum of squares; Adj SS—extra sum of squares; Seq MS—sequential mean squares; F—F-test and P—percent contribution.

cally highly significant. However sliding velocity (A) factor ($P = 14.19\%$), ($B \times C$) interaction between normal load \times filler content ($P = 8.18\%$), interaction ($A \times B$) between sliding velocity \times normal load ($P = 5.99\%$) and interaction ($A \times C$) between sliding velocity \times filler content ($P = 2.11\%$) have lesser effect on specific wear rate as error value ($P = 14.25\%$) was higher side hence less significant. From the analysis of ANOVA and response **Table 9** of the S/N ratio for specific wear rate, it was observed that the normal load has major impact on specific wear rate followed by filler content and sliding velocity.

The influence of each control factor on the specific wear rate was analyzed with a the main effect plot as shown in **Figure 4(a)** and an interaction plot as shown in **Figure 4(b)**. From the analysis it was observed that the control factor normal load (B) has major impact on the specific wear rate followed by the filler content (C) and sliding velocity (A). It means that for Al_2O_3 filled hybrid composites, with the increases of the sliding velocity and normal load the specific wear rate decreases. It was also observed that as the filler content (Al_2O_3) increases up to 10 wt% the specific wear rate decreases and further increase in filler content increases the specific wear rate. Analysis of these results leads to the conclusion that optimal values of the parameters for minimizing the wear rate when the sliding velocity was at level 3, normal load was at level 3 and the filler content was at level 2.

3.3.2. ANOVA and Effects of Factors on Coefficient of Friction

From the ANOVA **Table 10** for the coefficient of friction that the filler content (C) factor ($P = 51.08\%$) and interaction of normal load ($B \times C$) filler content ($P = 16.47\%$) have significant influence on the coefficient of friction. However the interaction ($A \times C$) between sliding velocity \times filler content ($P = 9.92\%$), interaction between ($A \times B$) sliding velocity \times normal load ($P = 5.55\%$), normal load (B) factor ($P = 2.23\%$) and sliding velocity ($P = 1.39\%$) do not have a significant effect both physically and statistical on coefficient of friction as their values were quite smaller than error ($P = 13.33\%$). So they were neglected. From the analysis of ANOVA and response **Table 11** of the S/N ratio of coefficient of friction, it was observed that the control parameter filler content (C) has a major impact on coefficient of friction followed by normal load and sliding velocity.

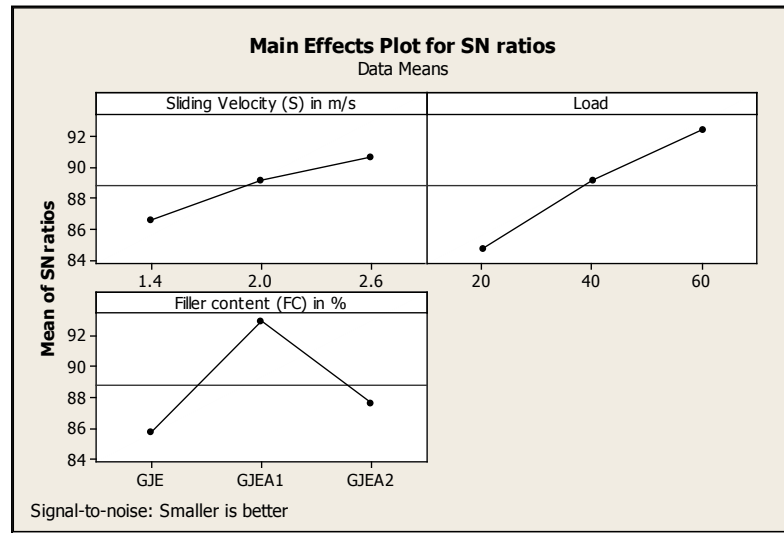
The influence of each control factor on the coefficient of friction was analyzed with a main effect plot as shown in **Figure 4(a)** and an interaction plot as shown in **Figure 4(b)**. From the analysis of ANOVA and response **Table 11** of the S/N ratio for coefficient of friction, it was observed that the control factor Al_2O_3 as a filler content (C) has major impact on the coefficient of friction. It means that for aluminum oxide filled hybrid composites, with the increases of the filler content from 0 wt% to 10 wt% coefficient of friction decreases and from 10 wt% to 15 wt% coefficient of friction increases. The same trend was observed for sliding velocity but the variation was very less, so the influence of sliding velocity on coefficient of friction was neglected. With the increase of normal load coefficient of friction increases due to thin transfer layer between the sliding materials formed because of plastic deformation of the epoxy and broken E-glass/jute fibers along with the Al_2O_3 fillers results in the easy shear during sliding [25]. Analysis of these results leads to the conclusion that optimal values of the parameters for minimizing the coefficient of friction when the sliding velocity and filler content were at level 2 and the normal load was at level 1.

3.3.3. Surface Morphology of Al_2O_3 Filled Hybrid Composites

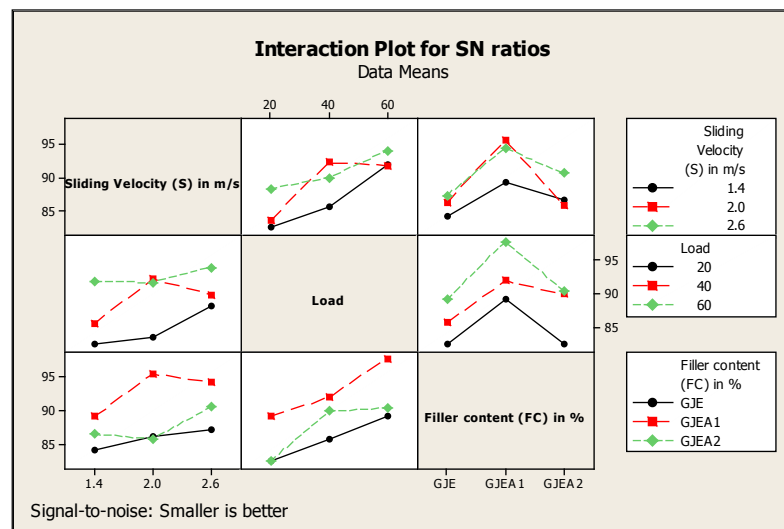
When compared with sliding velocity and filler content the effect of normal load on specific wear rate was more

Table 9. Response table for specific wear rate of Al_2O_3 filled hybrid composites.

Level	Control Factors		
	A	B	C
1	86.55	84.73	85.82
2	89.14	89.18	92.94
3	90.67	92.46	87.61
Delta	4.12	7.73	7.12
Rank	3	1	2



(a)



(b)

Figure 4. Effect of (a) control factors; (b) Interaction of factors on specific wear rate of Al₂O₃ filled hybrid composites.

Table 10. ANOVA table for COF of Al₂O₃ filled hybrid composites.

Source	DF	Seq SS	Adj SS	Adj MS	Test F	P (%)
A	2	0.003	0.003	0.002	0.418	1.39
B	2	0.005	0.005	0.003	0.668	2.23
C	2	0.123	0.123	0.061	15.325	51.08
A*B	4	0.013	0.013	0.003	0.832	5.55
A*C	4	0.024	0.024	0.006	1.488	9.92
B*C	4	0.040	0.040	0.010	2.470	16.47
Residual Error	8	0.032	0.039	0.005		13.33
Total	26	0.240				100.00

DF—degree of freedom; Seq SS—sequential sum of squares; Adj SS—extra sum of squares; Seq MS—sequential mean squares; F—F-test and P—percent contribution.

Table 11. Response table for COF of Al₂O₃ filled hybrid composites.

Level	Control Factors		
	A	B	C
1	7.815	8.395	7.816
2	8.105	7.679	9.699
3	7.797	7.644	6.203
Delta	0.308	0.751	3.496
Rank	3	2	1

for Al₂O₃ filler filled hybrid composite as seen from main effect plot **Figure 4(a)**, So SEM images were selected for different normal load conditions. **Figures 6(a)-(c)** show the SEM images for normal load 20 N, 40 N and 60 N conditions respectively for 10 wt% of Al₂O₃ filled epoxy composites. The micrograph in **Figure 6(a)** shows the wedge debris where more amount of epoxy matrix has been worn out which results in maximum wear. Few fibers were exposed as shown in **Figure 6(b)** due to temperature rise between the surfaces and surface matrix layer has been worn out. When compared with both the samples (a & b) the fibers were not exposed and matrix worn out from the surface of sample (c) where less which results in less wear as shown in **Figure 6(c)**.

Similarly, when compared with sliding velocity and normal load the effect of filler content (Al₂O₃) on coefficient of friction was more as seen from main effect plot **Figure 5(a)**, So SEM images were selected for different filler content of hybrid composites. The worn surface of **Figure 6(d)** unfilled hybrid composite and **Figure 6(f)** 15 wt% of Al₂O₃ filled hybrid composite show the plastic deformation of matrix, fibers were exposed and breakage of fibers which increases coefficient of friction due to rubbing of fiber and matrix with the disc surface [25]. The SEM for **Figure 6(e)** 10 wt% of Al₂O₃ filled hybrid composite sample show breakage of fiber and matrix due to weak bonding strength results in less coefficient of friction [16].

4. Confirmation Experiments

The confirmation experiment was conducted to validate the inference drawn during the analysis phase and considered as a final test in design of experiment process. The new set of factor setting A₂B₃C₂ was considered to predict the coefficient of friction for confirmation experiment. The estimated S/N ratio for coefficient of friction can be calculated with the help of following predictive Equation (5) [24].

$$\bar{\eta}_{HFRE1} = \bar{T} + (\bar{A}_2 - \bar{T}) + (\bar{B}_3 - \bar{T}) + [(\bar{A}_2\bar{B}_3 - \bar{T}) - (\bar{A}_2 - \bar{T}) - (\bar{B}_3 - \bar{T})] + (\bar{C}_2 - \bar{T}) \quad (5)$$

where $\bar{\eta}_{HFRE1}$ —predicted average; \bar{T} —overall experimental average and $\bar{A}_2\bar{B}_3$ and \bar{C}_2 —mean response for factors and interactions at designed levels. By combining all the terms the above Equation (5) reduces to

$$\bar{\eta}_{HFRE1} = \bar{A}_2\bar{B}_3 + \bar{C}_2 - \bar{T} \quad (6)$$

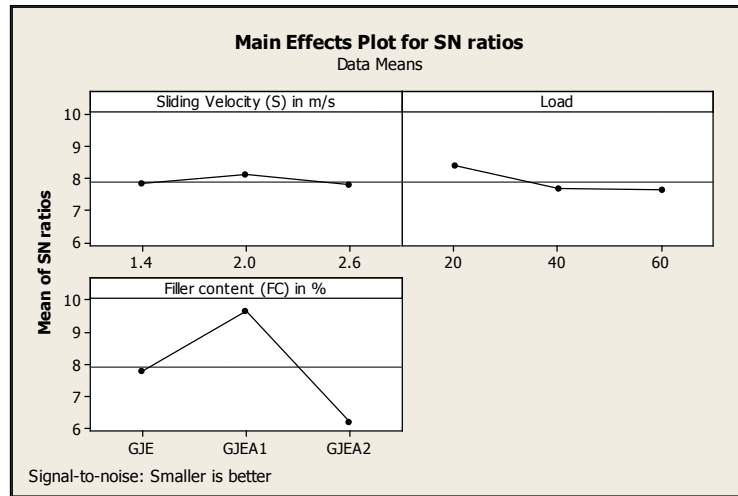
Similarly a prediction Equation (7) was developed for estimating S/N ratio of specific wear rate

$$\bar{\eta}_{HFRE2} = \bar{T} + (\bar{A}_2 - \bar{T}) + (\bar{B}_1 - \bar{T}) + [(\bar{A}_2\bar{B}_1 - \bar{T}) - (\bar{A}_2 - \bar{T}) - (\bar{B}_1 - \bar{T})] + (\bar{C}_2 - \bar{T}) \quad (7)$$

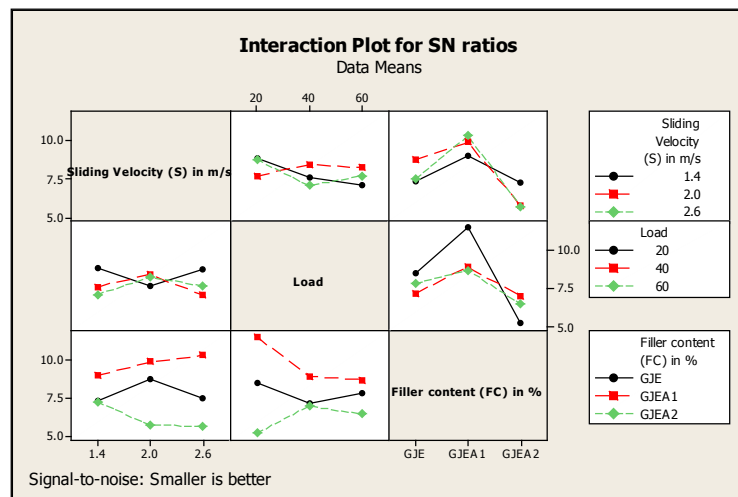
where $\bar{\eta}_{HFRE2}$ —predicted average; \bar{T} —overall experimental average and $\bar{A}_2\bar{B}_1$ \bar{C}_2 —mean response for factors and interactions at designated levels. By combining all the terms the above Equation (7) reduces to

$$\bar{\eta}_{HFRE2} = \bar{A}_2\bar{B}_1 + \bar{C}_2 - \bar{T} \quad (8)$$

For each of performance measures an experiment was conducted for different combination of factors and results were compared with those obtained from the predictive equation for specific wear rate (**Table 12**) and for coefficient of friction (**Table 13**) [24]. The above Equations (6) and (8) were capable of predicting the coefficient of friction and specific wear rate to the acceptable level of accuracy. An error for the S/N ratio of the coefficient of friction and for the S/N ratio of the specific wear rate was observed and shown in **Table 12** and **Table 13**. However if number of observations of performance characteristics were increased further these errors can be reduced.



(a)



(b)

Figure 5. Effect of (a) control factors; (b) Interaction on COF of Al₂O₃ filled hybrid composites.

Table 12. Results of the confirmation experiments for the Specific wear rate.

S/N ratio for specific wear rate (db) of hybrid composites/Level	Optimal Control Parameters		Error (%)
	Prediction A ₂ B ₁ C ₂	Experimental A ₂ B ₁ C ₂	
Bone Powder	93.2519	97.8461	4.92
Al ₂ O ₃	90.1310	86.3159	4.23

Table 13. Results of the confirmation experiments for the Coefficient of friction.

S/N ratio for coefficient of friction (db) of hybrid composites/Level	Optimal Control Parameters		Error (%)
	Prediction A ₂ B ₃ C ₂	Experimental A ₂ B ₃ C ₂	
Bone Powder	6.79363	6.4783	4.64
Al ₂ O ₃	9.21697	9.5324	3.42

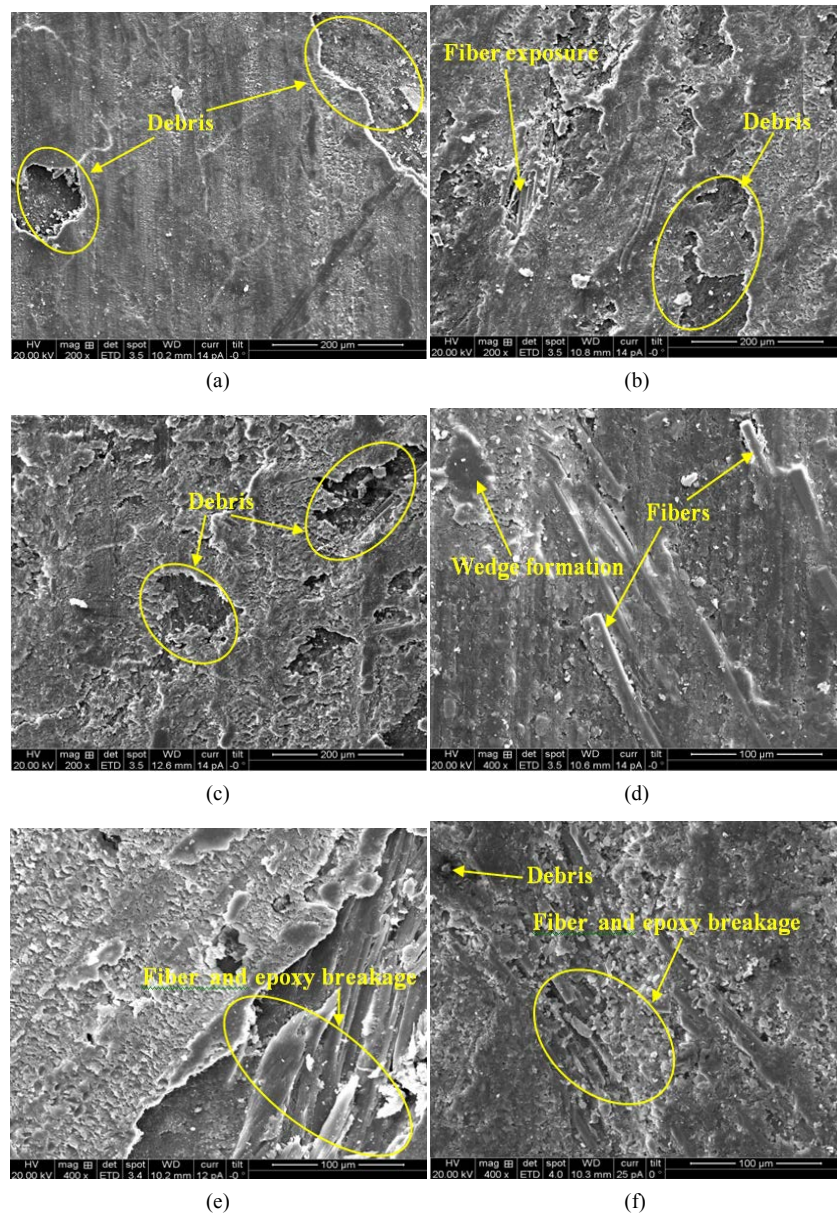


Figure 6. SEM images of composites for Al_2O_3 filled hybrid composites.

5. Conclusions

From the results and discussion the following conclusions can be made:

- Fabrication of hybrid composites consisting of E-glass/jute fiber reinforcement in epoxy with Al_2O_3 and bone powder filler was done successfully. The incorporation of Al_2O_3 and bone powder as secondary phase in the epoxy matrix improved the tribological characteristics;
- Design of experiments approach by Taguchi method enabled to successfully analyze the friction and wear behavior of the composites with sliding velocity, normal load and filler content as test variable;
- The wear resistance was increased for the addition of 10 wt% of Al_2O_3 and bone powder filled composites. Normal load for Al_2O_3 and filler content for bone powder were the main factors that had the highest physical and statistical significance in influencing the specific wear rate;
- The coefficient of friction decreased for the addition of 10 wt% of Al_2O_3 but it increased for bone powder filled hybrid composites due to weak bonding strength of composite material, and layers were transformed

between the sliding materials. Filler content was the main factor that had the highest physical and statistical significance in influencing the coefficient of friction for Al₂O₃ and bone powder filled composites;

- The predictive equations based on Taguchi approach were successfully used for the prediction of effect of various factors and predicted results were consistent with experimental observations. SEM studies of worn surfaces supported the involved mechanisms and indicated micro-cracking, debris, wear track, exposure of fibers, fiber breakage and wedge formation.

References

- [1] Bagci, M., Imrek, H. and Khalfan, O.M. (2015) Optimization of Test Parameters That Influence Erosive Wear Behaviors of Glass Fiber-Reinforced Epoxy Composites by Using the Taguchi Method. *Journal of Tribology*, **137**, 1-7.
- [2] Sudeepan, J., Kumar, K., Barman, T.K. and Sahoo, P. (2014) Study of Friction and Wear of ABS/Zno Polymer Composite Using Taguchi Technique. *Procedia Materials Science*, **6**, 391-400. <http://dx.doi.org/10.1016/j.mspro.2014.07.050>
- [3] Sen, T.J. and Reddy, H.N. (2014) Efficacy of Bio-Driven Jute FRP Composite Based Technique for Shear Strength Retrofitting of Reinforced Concrete Beams and Its Comparative Analysis with Carbon and Glass FRP Shear Retrofitting schemes. *Sustainable Cities and Society*, **13**, 105-124. <http://dx.doi.org/10.1016/j.scs.2014.04.010>
- [4] Shukla, D.K., Kasisomayajula, S.V. and Parameswaran, V. (2008) Epoxy Composites Using Functionalized Alumina Platelets as Reinforcements. *Composites Science and Technology*, **68**, 3055-3063. <http://dx.doi.org/10.1016/j.compscitech.2008.06.025>
- [5] Scarponi, C. and Messano, M. (2015) Comparative Evaluation between E-Glass and Hemp Fiber Composites Application in Rotorcraft Interiors. *Composites Part B: Engineering*, **69**, 542-549. <http://dx.doi.org/10.1016/j.compositesb.2014.09.010>
- [6] AlMaadeed, M.A., Nogellova, Z., Micusik, M., Novak, I. and Krupa, I. (2014) Mechanical, Sorption and Adhesive Properties of Composites Based on Low Density Polyethylene Filled with Date Palm Wood Powder. *Mat and Design*, **53**, 29-37. <http://dx.doi.org/10.1016/j.matdes.2013.05.093>
- [7] AlMaadeed, M.A., Nogellova, Z., Janigova, I. and Krupa, I. (2014) Improved Mechanical Properties of Recycled Linear Low-Density Polyethylene Composites Filled with Date Palm Wood Powder. *Mat and Design*, **58**, 209-216. <http://dx.doi.org/10.1016/j.matdes.2014.01.051>
- [8] Shah, D.U. (2014) Natural Fibre Composites: Comprehensive Ashby-Type Materials Selection Charts. *Mat and Design*, **62**, 21-31. <http://dx.doi.org/10.1016/j.matdes.2014.05.002>
- [9] Nabinejad, O., Sujan, D., Rahman, M.E. and Davies, I.J. (2015) Effect of Oil Palm Shell Powder on the Mechanical Performance and Thermal Stability of Polyester Composites. *Mat and Design*, **65**, 823-830. <http://dx.doi.org/10.1016/j.matdes.2014.09.080>
- [10] Akil, H.M., Santulli, C., Sarasini, F., Tirillo, J. and Valente, T. (2014) Environmental Effects on the Mechanical Behaviour of Pultruded Jute/Glass Fibre-Reinforced Polyester Hybrid Composites. *Composites Science and Technology*, **94**, 62-70. <http://dx.doi.org/10.1016/j.compscitech.2014.01.017>
- [11] Cakir, O.A., Sarikanat, M., Tufekci, H.B., Demirci, C. and Erdogan, U.H. (2014) Physical and Mechanical Properties of Randomly Oriented Coir Fiber-Cementitious Composites. *Composites Part B: Engineering*, **61**, 49-54. <http://dx.doi.org/10.1016/j.compositesb.2014.01.029>
- [12] Asuke, F., Aigbodion, V.S., Abdulwahab, M., Fayomi, O.S.I., Popoola, A.P.I., Nwoyi, C.I. and Garba, B. (2012) Effects of Bone Particle on the Properties and Microstructure of Polypropylene/Bone Ash Particulate Composites. *Results in Physics*, **2**, 135-141. <http://dx.doi.org/10.1016/j.rinp.2012.09.001>
- [13] Srivastava, V.K. and Pawar, A.G. (2006) Solid Particle Erosion of Glass Fibre Reinforced Flyash Filled Epoxy Resin Composites. *Composites Science and Technology*, **66**, 3021-3028. <http://dx.doi.org/10.1016/j.compscitech.2006.02.004>
- [14] Akil, H.M., Cheng, L.W., Mohd Ishak, Z.A., Bakar, A.A. and Rahman, M.A.A. (2009) Water Absorption Study on Pultruded Jute Fibre Reinforced Unsaturated Polyester Composites. *Composites Science and Technology*, **69**, 1942-1948. <http://dx.doi.org/10.1016/j.compscitech.2009.04.014>
- [15] Suresha, B., Devarajaiah, R.M., Pasang, T. and Ranganathaiah, C. (2013) Investigation of Organo-Modified Montmorillonite Loading Effect on the Abrasion Resistance of Hybrid Composites. *Materials & Design*, **47**, 750-758. <http://dx.doi.org/10.1016/j.matdes.2012.12.056>
- [16] Baradeswarana, A., Elayaperumal, A. and Issac, R.F. (2013) A Statistical Analysis of Optimization of Wear Behaviour of Al-Al₂O₃ Composites Using Taguchi Technique. *Procedia Engineering*, **64**, 973-982. <http://dx.doi.org/10.1016/j.proeng.2013.09.174>
- [17] Siddhartha, Patnaik, A. and Bhatt, A.D. (2011) Mechanical and Dry Sliding Wear Characterization of Epoxy-TiO₂ Par-

- ticulate Filled Functionally Graded Composites Materials Using Taguchi Design of Experiment. *Materials & Design*, **32**, 615-627. <http://dx.doi.org/10.1016/j.matdes.2010.08.011>
- [18] Ravindran, P., Manisekar, K., Narayanasamy, P., Selvakumar, N. and Narayanasamy, R. (2012) Application of Factorial Techniques to Study the Wear of Al Hybrid Composites with Graphite Addition. *Materials & Design*, **39**, 42-54. <http://dx.doi.org/10.1016/j.matdes.2012.02.013>
- [19] Sudeep, S.D. and Rangaswamy, T. (2014) Effect of Fillers on E-Glass/Jute Fiber Reinforced Epoxy Composites. *International Journal of Engineering Research and Applications*, **4**, 118-123.
- [20] Nirmal, U., Hashim, J. and Megat Ahmad, M.M.H. (2015) A Review on Tribological Performance of Natural Fibre Polymeric Composites. *Tribology International*, **83**, 77-104. <http://dx.doi.org/10.1016/j.triboint.2014.11.003>
- [21] Ahmad, K.Z.K., Ahmad, S.H., Tarawneh, M.A. and Apte, P.R. (2012) Evaluation of Mechanical Properties of Epoxy/Nanoclay/Multi-Walled Carbon Nanotube Nanocomposites Using Taguchi Method. *Procedia Chemistry*, **4**, 80-86. <http://dx.doi.org/10.1016/j.proche.2012.06.012>
- [22] Ram Prabhu, T. (2015) Effects of Solid Lubricants, Load, and Sliding Speed on the Tribological Behavior of Silica Reinforced Composites Using Design of Experiments. *Materials & Design*, **77**, 149-160. <http://dx.doi.org/10.1016/j.matdes.2015.03.059>
- [23] Uvaraja, V.C., Natarajan, N., Rajendran, I. and Sivakumar, K. (2013) Tribological Behavior of Novel Hybrid Composite Materials Using Taguchi Technique. *Journal of Tribology*, **135**, 021101-12. <http://dx.doi.org/10.1115/1.4023147>
- [24] Patnaik, A., Abdulla, Md., Satapathy, A., Biswas, S. and Satapathy, B.K. (2010) A Study on a Possible Correlation between Thermal Conductivity and Wear Resistance of Particulate Filled Polymer Composites. *Mat and Design*, **31**, 837-849. <http://dx.doi.org/10.1016/j.matdes.2009.07.046>
- [25] Yallew, T.B., Kumar, P. and Singh, I. (2014) Sliding Wear Properties of Jute Fabric Reinforced Polypropylene Composites. *Procedia Engineering*, **97**, 402-411. <http://dx.doi.org/10.1016/j.proeng.2014.12.264>